

Supersolid and pair correlations of extended Jaynes-Cummings-Hubbard model on the triangular and one dimensional lattices

Lijuan Guo,¹ Sebastian Greschner,² Siyu Zhu,¹ and Wanzhou Zhang¹

¹*College of Physics and Optoelectronics, Taiyuan University of Technology, Shanxi 030024, China*

²*Institut für Theoretische Physik, Leibniz University Hannover, Appelstr. 2, DE-30167 Hannover, Germany*

(Dated: October 15, 2019)

We study the extended Jaynes-Cummings-Hubbard model on the triangular and one-dimensional cavity lattices. By using mean-field and density matrix renormalization group methods, we observe various types of solids with different density patterns and find evidences for light supersolids. The triangular lattices exhibit extended supersolid regions in the phase diagram. Apart from the hole-excited supersolid phase, we also see an additional supersolid phase. Besides, novel pair correlations are found due to the interplay between the atoms in the cavities and atom-photon interaction. On the one-dimensional lattices both for the hardcore and softcore models, we find indications for a particle-excited or a hole-excited supersolid phase emerging around the solid phase. Beats emerge within the SS phase for the density-density correlation in both hardcore and softcore models. The results are helpful in guiding experimentalists in realizing novel quantum phases on optical lattices.

I. INTRODUCTION

Searching for novel supersolids (SS) and exploring their nature is an interesting topic in the field of condensed matter physics [1–4]. The controllable ultracold-atom system in optical lattices provides a pristine and convenient platform to realize such tasks [5, 6]. Multi-component systems of ultracold atoms are possible candidates to host the SS phase [7–10]. The Jaynes-Cummings-Hubbard (JCH) model is a particular two component system, which is a combination of the JC model [11, 12] and the coupled cavities where each cavity contains a two-level atom.

Experimentally, the JCH model can be realized by a coupled-transmission-line resonator [13] or trapped ions [14]. Analytically, the mean-field (MF) theory [15, 16], the Ginzburg-Landau theory [17], the strong-coupling random-phase approximation method [18] are all used to study the properties of the JCH model. Furthermore, the correlation and critical exponents of the JCH model can be obtained by many reliable numerical methods, such as, the density matrix renormalization group algorithm(DMRG) [19, 20] and the quantum Monte-Carlo(QMC) method [21, 22].

Moreover, several interesting topics concerning the JCH model have been studied, which include fractional quantum Hall physics [23], quantum transport [24], quantum-state transmission [25], on-site disorder [16, 26] and the interesting quantum phase transition between the superfluid (SF) phase and the Mott-insulator (MI) phase [12].

All of these previous works ignored the interaction between atoms. Until recently, the light supersolid was found in the Dicke model of a cavity modeled by quantum electrodynamics coupled with a one dimensional Rydberg lattice with the next repulsion [27]. However, since the photon hopping between each cavity was not considered, it remains unclear whether or not the photon hopping will break the supersolid phase. At the same

time, the regimes of the SS phase by a hole or particle-excited mechanism is very narrow in the phase diagram. It is interesting to study the extended JCH model on the triangular cavity lattices and check whether the additional SS exists in the phase diagram, which may be stabilized by an order-by-disorder mechanism as discussed in Refs. [28–30] in the context of Bose-Hubbard models on triangular lattices.

On the other hand, in Ref. [31] a light supersolid in the extended JCH model on the square lattices was found by MF methods. The authors pointed out that the supersolid phase needed to be confirmed by other large scale numerical methods, as the results from the MF method are not very reliable. Therefore, it is necessary to study the extended JCH model on the one dimensional lattices, which is also a bipartite lattice but can be tackled easier by means of the numerically exact DMRG method.

In this work, we firstly study the extended JCH model on the triangular lattices, just by showing the mean-field phase diagrams, in which the regimes of the SS phase is wider than those of the one dimensional lattices. The phase transitions between different phases are also studied. Some results are also confirmed by the DMRG method of the model on the triangular zigzag ladder. Besides, a phase with dominant pair correlations is found by the DMRG method.

Furthermore, the extended JCH model is studied on the one dimensional lattices and the SS phase appears around the tips of the solid for both the softcore and hardcore models. The stability of the SS phase is also checked by a finite size scaling analysis with the DMRG method. The experimental signatures of the SS phase are also shown by the momentum distribution and correlation. Interestingly, beats emerge within the SS phase for the density-density correlation.

The outline of this work is as follows. Section II shows the JCH model and the Hamiltonian. Section III shows the MF and the DMRG methods. Section IV shows the results of the hardcore JCH model on the triangular lat-

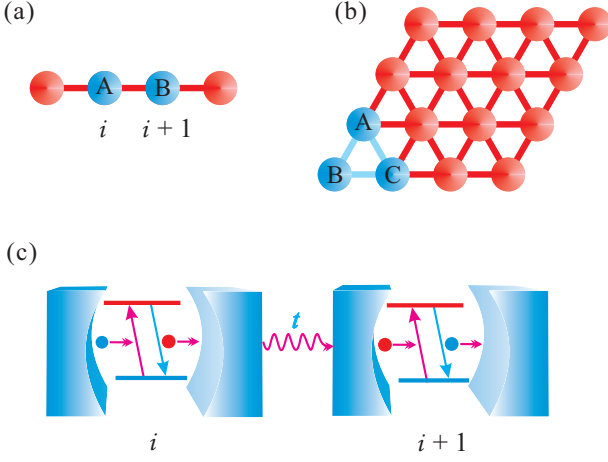


FIG. 1. (a) One dimensional lattices, each ball denotes a cavity. (b) A triangular cavity lattices. (c) A photon denoted by a red symbol is tunneling between two different cavities which are labeled by i and $i+1$, and t is the hopping strength. In each cavity, the atom has two energy levels which are labeled by two separated horizontal lines.

tices by MF method and the triangular zigzag ladder by DMRG method. Section V shows the results of the JCH model on the 1D lattice for both the hardcore and soft-core models by the MF method and the DMRG method. Concluding comments are made in Section VI.

II. MODEL AND HAMILTONIAN

Figs. 1 (a) and (b) show the JCH model on the one dimensional and triangular cavity lattices. For convenience, we decompose each unit cell into two (three) sublattices labeled by A and B (A , B and C).

On each cavity site i , the two-level atom is contained. The on-site coupling between the photons and the atom on each site i can be described by the JC Hamiltonian H_i^{JC}

$$H_i^{JC} = \omega n_i^a + \varepsilon n_i^\sigma + \beta(a_i^\dagger \sigma_i + a_i \sigma_i^\dagger), \quad (1)$$

where ω is the frequency of the mode of the photon creation and annihilation operators at lattice site i , ε is the transition frequency between two energy levels, $n_i^a = a_i^\dagger a_i$ and $n_i^\sigma = \sigma_i^\dagger \sigma_i$ are the photon number and the number of excitations of the atomic levels, respectively. a_i^\dagger and a_i are the photon creation and annihilation operators at lattice site i , Pauli matrices σ_i^\dagger (σ_i) represent the raising (lowering) operator, and β is the atom-photon coupling strength. As shown in Fig. 1 (c), $a_i \sigma_i^\dagger$ means that a photon is absorbed and an atom excitation forms simultaneously.

The extended JCH model includes a dipole interaction term with strength V , and photon tunneling term with t between cavities. The Hamiltonian is defined as

$$H = \sum_i (H_i^{JC} - \mu n_i) - t \sum_{\langle i,j \rangle} (a_i^\dagger a_j + \text{H.c.}) + \sum_{\langle i,j \rangle} V n_i^\sigma n_j^\sigma, \quad (2)$$

where the total number of excitations is $\rho \equiv \sum_i n_i = \sum_i (n_i^\sigma + n_i^a)$, μ is the chemical potential, t is the hopping amplitude of photons between a pair of neighboring lattice sites i and j and V is the nearest-neighbor interactions between the atoms.

In the limit of a dominant atom-photon coupling $\beta \gg V, t$ for fillings $\rho < 1$ one may project model (2) to its low-energy-subspace composed of sites with on-site singlets ($|g, 1\rangle_x - |e, 0\rangle_x$)/ $\sqrt{2}$ and empty sites $|g, 0\rangle_x$. After identification with the states $|1\rangle_x^b$ and $|0\rangle_x^b$ of a (hardcore) Bose-Hubbard model we may, hence, as a first order approximation map model (2) to the following Hamiltonian

$$H_{BH} = \sum_i (-\beta - \mu) n_i^b - \frac{t}{2} \sum_{\langle i,j \rangle} (b_i^\dagger b_j + \text{H.c.}) + \frac{V}{4} \sum_{\langle i,j \rangle} n_i^b n_j^b, \quad (3)$$

with bosonic annihilation (creation) operators b_i (b_i^\dagger) and $n_i^b = b_i^\dagger b_i$. The properties of model (3) have been studied extensively for various lattice geometries in for example Refs. [28, 29, 32–34]. In the following we focus on the properties of the model (2) in the regime $t < V \lesssim \beta$.

III. METHODS

A. Cluster mean field method

The single-site MF has successfully predicted the SF-MI phase transition without long-range interaction ($V=0$) [35]. The cluster mean-field (CMF) will be more reasonable to predict the physics in the interaction systems ($V \neq 0$) [36–39]. The basic idea is to divide the system into N_c unit cells, and each unit cell contains nc sites. The Hamiltonians within each cell are treated exactly and the Hamiltonians between each cell are approximated by $AB \approx A\langle B \rangle + \langle A \rangle B - \langle A \rangle \langle B \rangle$.

The total Hamiltonian can be considered as a sum over the local Hamiltonians on each unit cell, which contain the parts treated exactly H_{in}^c and the CMF Hamiltonian H_{MF}^c as follows:

$$H = \sum_{c=1}^{N_c} (H_{in}^c + H_{MF}^c), \quad (4)$$

The Hamiltonian H_{in}^c can be expressed as:

$$H_{in}^c = -zt \sum_{i,j \in c} (a_i^\dagger a_j + \text{H.c.}) + zV \sum_{i,j \in c} n_i^\sigma n_j^\sigma + \sum_{i \in c} h_i \quad (5)$$

where $h_i = -\mu_p n_i^a - (\Delta + \mu_s) n_i^\sigma + \beta(\sigma_i^\dagger a_i + a_i^\dagger \sigma_i)$. The chemical potential of photons is μ_p and the chemical potential of atoms is μ_s , and the different labels of chemical potential are convenient to test our codes. In real simulations, $\mu_p = \mu_s = \mu - \omega$, $\Delta = \omega - \varepsilon$, and Δ are maintained at zero for convenience.

The Hamiltonian H_{MF}^c is given by:

$$H_{MF}^c = -qt \sum_{i,j \in ce} [(a_i^\dagger + a_i)\Psi_j + (a_j^\dagger + a_j)\Psi_i - 2\Psi_i\Psi_j] + qV \sum_{i,j \in ce} (n_i^\sigma \rho_j^\sigma + n_j^\sigma \rho_i^\sigma - \rho_i^\sigma \rho_j^\sigma), \quad (6)$$

where z is equal to 1, the chosen setting in Ref. [31], $q = z$ for the one-dimension lattices, $q = 2z$ for the triangular lattices, and $\Psi_i = \langle a_i \rangle$ is the superfluid order parameter, $\rho_i^\sigma = \langle n_i^\sigma \rangle$ is the number of atomic excitations. In the SF phase, Ψ_i is homogeneous between different lattice sites.

The solid or density wave orders denoted by $\Delta\rho^a$, $\Delta\rho^\sigma$, and $\Delta\Psi$ are defined by:

$$\Delta A = \frac{1}{nc} \sum_{i \in c} |A_i - \bar{A}|, \quad \bar{A} = \frac{1}{nc} \sum_{i \in c} \bar{A}_i. \quad (7)$$

We also define the total excitation $\rho = \rho^a + \rho^\sigma$ [12], and $\Delta\rho = \frac{1}{2}(\Delta\rho^a + \Delta\rho^\sigma)$. In the one dimensional lattices, a possible solid pattern (ρ_A, ρ_B) is equal to (0, 1) and denoted by SI. In the triangular lattices, (ρ_A, ρ_B, ρ_C) are equal to two possible patterns (0, 0, 1) and (0, 1, 1) respectively, which are denoted by SII and SIII. In the perfect SI, SII and SIII phases, $\Delta\rho$ is equal to 1/4, 2/9 and 2/9 with $t/\beta = 0$, respectively. We have verified that our results are stable under enlargement of clusters, such as a larger cluster with size 6 sites[37].

B. DMRG method

To confirm the results obtained by the CMF method, we also use the DMRG [40, 41] method to get the ground-state energy and the wave function with open boundary conditions keeping up to $m = 600$ matrixstates in the sector of a fixed number of excitations ρ . We calculate several observables and correlation-functions to characterize the various groundstate-phases.

The structural factor is defined to characterize the solid order [28–30, 42, 43].

$$S_k/L = \langle \rho_k^\sigma \rho_k^{\sigma^\dagger} \rangle, \quad (8)$$

where $\rho_k^\sigma = (1/L) \sum_{i=1}^L n_i^\sigma \exp(\sqrt{-1}ki)$. S_k/L has a peak at $k = \pi$ for the SI phase but for the triangular zigzag ladder, the location of the maximum S_k/L , labeled by S_k^m/L is not necessarily at $k = \pi$ (will be discussed). It should be noted that ρ and ρ^a can also be substituted into the above equation and both quantities can reflect the solid order. Another signal of the solid orders are the

TABLE I. Values of the order parameters for typical phases. “E” denotes exponentially decaying, “P” denotes power-law decaying.

	Solid	SF	SS	MI
Ψ	0	$\neq 0$	$\neq 0$	0
$\Delta\rho$	$\neq 0$	0	$\neq 0$	0
$\Delta\Psi$	0	0	$\neq 0$	0
$C_a(r)$	E	P	P	E
$C_n^a(r)$	E	P	P	E
S_k^m/L	$\neq 0$	0	$\neq 0$	0

power-law decaying of atom excitation correlation $C_n^\sigma(r)$ and photon density correlation $C_n^a(r)$, defined by

$$C_n^\sigma(r) = \langle n_i^\sigma n_{i+r}^\sigma \rangle - \langle n_i^\sigma \rangle \langle n_{i+r}^\sigma \rangle, \quad (9)$$

$$C_n^a(r) = \langle n_i^a n_{i+r}^a \rangle - \langle n_i^a \rangle \langle n_{i+r}^a \rangle.$$

In some regimes, the above correlations emerge in the shape of beats [44, 45].

The superfluid order could be denoted by non-integer fillings and power-law decaying of the non-diagonal correlation:

$$C_a(r) = \langle a_i^\dagger a_{i+r} \rangle. \quad (10)$$

The Fourier transform of the $C_a(r)$, namely, the momentum distribution is defined as

$$n(k) = \frac{1}{L} \sum_{i,j} \langle a_i^\dagger a_j \rangle \exp(\sqrt{-1}k(i-j)), \quad (11)$$

which was observed experimentally [5].

Besides the usual single particle tunneling correlation, pairing-correlations may be defined as

$$C_a^\sigma(r) = \langle a_i^\dagger \sigma_i^\dagger \sigma_{i+r} a_{i+r} \rangle,$$

$$C_a^a(r) = \langle a_i^\dagger a_{i+1}^\dagger a_{i+r} a_{i+r+1} \rangle, \quad (12)$$

$$C_\sigma^\sigma(r) = \langle \sigma_i^\dagger \sigma_{i+1}^\dagger \sigma_{i+r} \sigma_{i+r+1} \rangle.$$

In Tab. I, we show the values or the behaviors of the order parameters for several typical phases.

IV. THE RESULTS ON THE TRIANGULAR LATTICES

A. The CMF results on the triangular lattices

Firstly, in the limit $t = 0$ and large $\beta \gg V$, where Eq. (3) is valid, the energy per unit cell is

$$E_\Delta = \sum_i [-\beta - \mu] n_i^b + \frac{3V}{4} (n_A^\sigma n_B^\sigma + n_B^\sigma n_C^\sigma + n_C^\sigma n_A^\sigma). \quad (13)$$

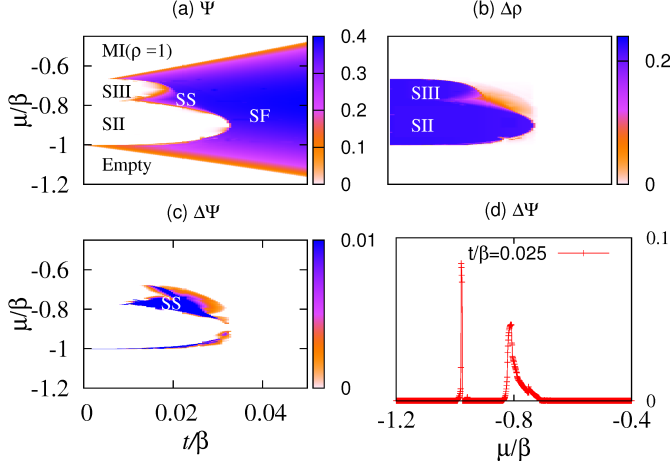


FIG. 2. Phase diagrams and the detailed description of $\Delta\Psi$ for the extended JCH model on triangular lattices with $V/\beta = 0.4$ by the CMF method. (a) The SF order Ψ . (b) The solid order $\Delta\rho$. (c) The SS order $\Delta\Psi$. (d) $\Delta\Psi$ vs μ/β with $t/\beta = 0.025$.

where n_A^σ, n_B^σ and n_C^σ are the number of excitations on the sublattice $i = A, B$, and C , as shown in Fig. 1(b). By increasing μ , the density ρ will undergo platforms with values of $1/3, 2/3$ with solid patterns ($n_A^\sigma, n_B^\sigma, n_C^\sigma$) are $(0, 0, 1)$ and $(0, 1, 1)$, which have special interest. In a grand-canonical ensemble, the two solid phases exhibit a direct transition at $t = 0$ with all states with $1/3 < \rho < 2/3$ being macroscopically degenerate in this classical limit. The hardcore Bose-Hubbard model on the triangular lattices has been studied in Refs. [28, 29, 42, 43] on triangular lattices for a finite hopping $|t| > 0$ and the emergence of supersolid phases stabilized by an order-by-disorder mechanism for intermediate fillings $1/3 < \rho < 2/3$ has been shown.

In our calculations, V/β is set to be 0.4 just as in Ref. [31], fixing $\beta = 1$ as the unit. In Fig. 2 we present the results of our CMF simulations for these parameters which show the two solid phases SII and SIII for a finite atom-photon coupling β in the limit of vanishing and small $t \ll \beta$. It is important to note, that for $t = 0$ as known for the Bose-Hubbard limit the two phases exhibit a first order transition with a macroscopic jump of density between the two platforms. Furthermore, as shown in Figs. 2 (a) and (b), due to the coupling between atoms and photons, the SII and SIII phases are not symmetric with $\mu/\beta = -0.77$, which is different from the particle hole symmetry of the hardcore bosons on the triangular lattices [28–30].

Interestingly, as shown in Fig. 2 (c), the SS phase appears between the SII and SIII phases with $\Delta\Psi \neq 0$. Between the two solids, the SS phase can be understood in terms of photon-tunneling breaking the degeneracy between the SII and SIII phases. Hence, the emergence of such a SS phase may be based on an order-by-disorder mechanism as conjectured for Bose-Hubbard

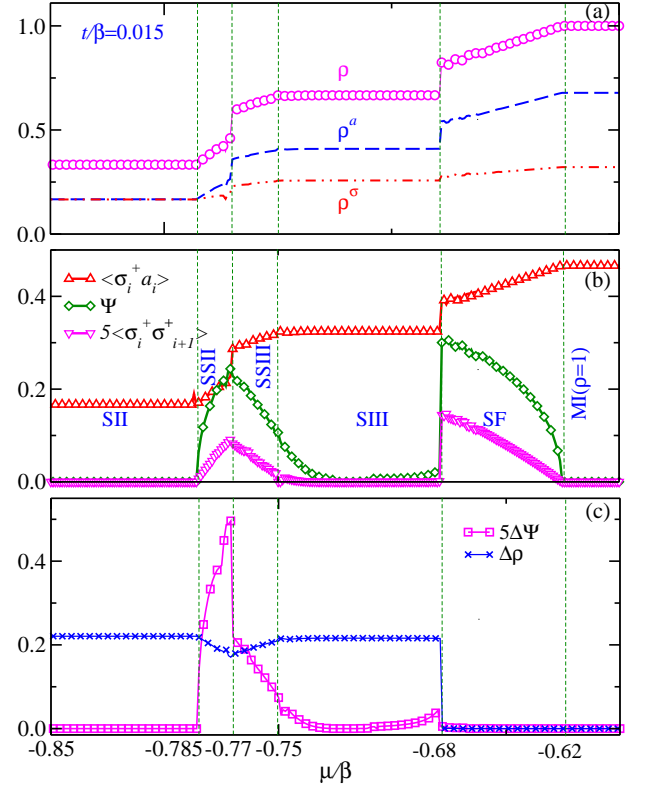


FIG. 3. MF method detailed description of (a) The density ρ . (b) The SF order Ψ , $\langle \sigma_i^\dagger a_i \rangle$, and $5\langle \sigma_i^\dagger \sigma_{i+r}^\dagger \rangle$. (c) Solid order $\Delta\rho$ and $\Delta\Psi$ vs μ/β with $V/\beta = 0.4$, $t/\beta = 0.015$ on the triangular lattices.

limit in Refs. [28–30].

In Fig. 2 (c), we also find that below the SII phase another SS phase emerges, which may be understood as hole-excited SS phase [27]. In Fig. 2 (d), $\Delta\Psi$ is shown along $t/\beta = 0.025$, and its values are not zero around $\mu/\beta = -1$ (hole-excited SS) and $\mu/\beta = -0.8$, respectively.

To illustrate the above results more detailed, we scan the phase diagram along the lines with different values of t/β . As an example, we choose $t/\beta = 0.015$ in Fig. 3. Starting at $\mu/\beta = -0.85$ and increasing μ/β to -0.785 , the system is in the SII phase with $\rho = 1/3$, $\Psi = 0$ and $\Delta\rho = 0.22$. With a further increase of μ/β , the three quantities Ψ , $\Delta\Psi$ and $\Delta\rho$ become nonzero continuously, and the system enters into a SS phase. Since this SS phase is understood from particle-doping on the SII phase, therefore, we denote it as a SSII phase.

By increasing μ/β to -0.77 , the quantities ρ and $\Delta\Psi$ jump to nonzero values and the system enters into another SS phase. This SS phase could be called SSIII, because it is formed by hole-doping on the solid SIII. The phase transition of SSII to SSIII is first order. This is consistent with previous work [46, 47], in which the two SS phases of hardcore bosons take place according to first-order transitions. By continued increase of μ/β to -0.68 , it is obvious that Ψ becomes nonzero, which

means that the first-order SIII-SF phase transition takes place.

In the two ends of the SIII phase with fixed density $\rho = 2/3$, i.e., around $\mu/\beta = -0.75$ and $\mu/\beta = -0.68$, both $\Delta\Psi$ and Ψ are very weak and might disappear with larger system sizes.

In previous works, the nearest [32] or the next to nearest [48] repulsive interactions are the necessary conditions for the formation of the supersolid. It should be noted that in our model, even though there is no interaction between photons, the light supersolid emerges, because the repulsion of atoms will cause the effect of repulsion between photons due to the atom-photon coupling. This effected atom-photons can be verified by calculation of the expectation values of $\sigma_i^\dagger a_i$ or $\sigma_i a_i^\dagger$. As shown in Fig. 3 (b), $\langle \sigma_i^\dagger a_i \rangle$ is nonzero even the system is in the SII, SIII, MI($\rho = 1$) phases, where $\Psi = 0$. The behaviors of $\langle \sigma_i^\dagger a_i \rangle \neq 0$ and $\langle \sigma_i^\dagger \sigma_{i+1}^\dagger \rangle \neq 0$ mean that a type of fluctuation with transitions between atom excitations and photons, remains in the system. Nonzero $\langle \sigma_i^\dagger \sigma_{i+1}^\dagger \rangle$ is shown in Fig. 3(b). Actually, the behaviors of $\langle a_i^\dagger a_{i+r}^\dagger \rangle$, will be discussed in the next subsection.

B. The DMRG results on the triangular zigzag ladder

Considering the region of the hole-doped SS phase which is found in triangular lattices by using the MF method is not broad enough to distinguish whether there exists such a SS phase or not. In general, the SS phases are fragile against quantum fluctuations. As the triangular zigzag ladder are easier to be calculated by the DMRG method, in this section, we use the DMRG method to simulate the triangular zigzag ladder to further verify the results of the triangular lattices by using the CMF theory is reliable.

An important difference between the quasi 1D ladder geometry and the 2D lattices is that in the triangular two-leg-ladder a further solid density wave phase at half-filling can be found corresponding to a pattern (0, 0, 1, 1) in addition to the solid phases at fillings $1/3$ and $2/3$. The emergence and properties of these solid phases for the Bose-Hubbard limit have been studied in various works, e.g. Refs. [33, 34].

Fig. 4(a) shows the equation of state ρ versus μ/β with system size $L = 96$, $t/\beta = 0.015$ and $V/\beta = 0.4$. For this set of parameters only the gapped phase at $1/3$ filling is visible, characterized by the plateau in the $\mu - \rho$ curve. For the limit $t \rightarrow 0$ gapped phases at $1/2$ and $2/3$ emerge as well (not shown). We observe a stable SS phase in the range about $1/3 < \rho < 2/3$ and a clear example will be discussed for $\rho = 0.42$. The hole-excited supersolid ($0.22 < \rho < 1/3$) and the particle-excited supersolid ($2/3 < \rho < 0.875$) are also found.

To discuss the supersolid, Fig. 4(b) and (c) show the structural factor S_k^m/L and the momentum distribution

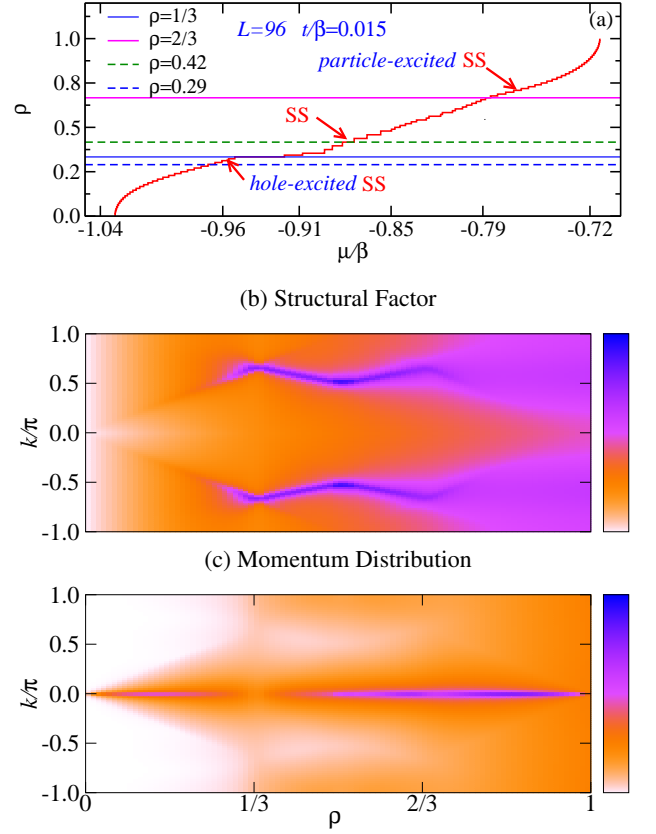


FIG. 4. DMRG method simulation of the hardcore extended JCH model on the triangular zigzag ladder with $V/\beta = 0.4$, $t/\beta = 0.015$, $L = 96$. (a) ρ vs μ/β . (b) The structural factor in the plane $(k/\pi, \rho)$. (c) The momentum distribution in the plane $(k/\pi, \rho)$.

$n(k)$ in the plane $(k/\pi, \rho)$, where both distributions have distinct peaks for $\rho \gtrsim 1/3$. Also for $\rho \lesssim 1/3$ we find indications for the presence of a hole-excited SS, which is also confirmed by the finite size scaling of the maximum structural factor in Fig. 5 and Fig. 6. In the interval $1/3 < \rho < 2/3$, clear peaks of both quantities observed means that the additional supersolid is found apparently. Particle-excited supersolid appears from the peaks for $\rho \gtrsim 2/3$.

An extrapolation to the thermodynamic limit of the maximum structural factor S_k , labeled by S_k^m , is performed with different sizes $L = 48, 96, 192$ in Fig. 5. In Fig. 5(b), the fitting of S_k^m/L at $\rho = 0.25, 0.29, 0.31$ (red triangular symbols) and $\rho = 0.42$ (blue diamond symbols) prove that the hole-excited SS phase and the additional SS phase, respectively, exist in the thermodynamic limit. Meanwhile, the particle-excited SS is also supported by nonzero S_k^m/L in the range $0.67 < \rho < 0.875$, for instance, $\rho = 0.71, 0.875$ shown in Fig. 5(c).

Interestingly, the $\mu - \rho$ curve shown in Fig. 4 (a) for $1/3 \gtrsim \rho \gtrsim 1/2$ exhibits a series of steps of two-particles $\Delta\rho = 2/L$. This property, signals the presence of a

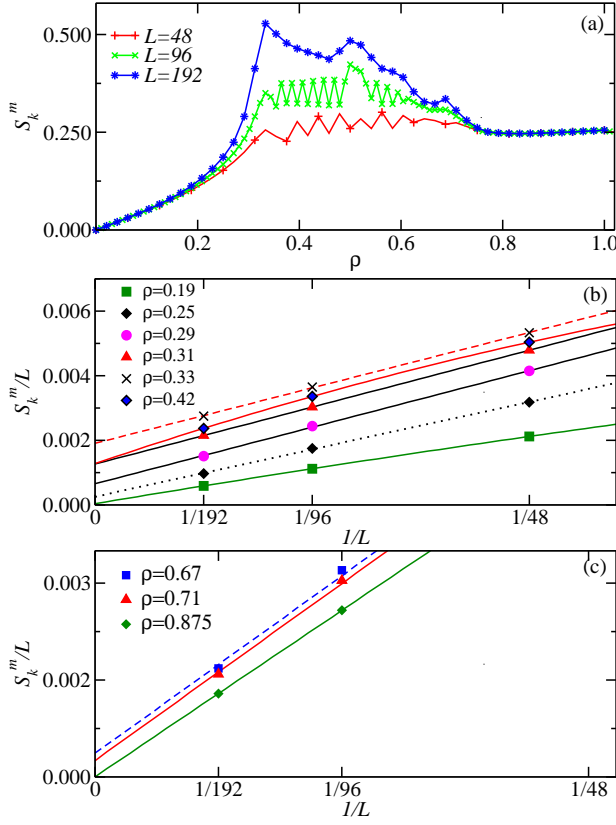


FIG. 5. Finite system size scaling of the maximum of the structural factor S_k^m . (a) S_k^m as function of ρ for three system sizes $L = 48, 96$ and 192 . (b) Extrapolation of S_k^m/L vs $1/L$, where $L = 48, 96, 192$ at $\rho = 0.19$ to 0.42 and (c) $\rho = 0.67$ to 0.875 , respectively.

pair-superfluid phase. Indeed, also the single-particle correlation-functions $C_a(r)$ in this region exhibit an exponential decay as can be seen in Fig. 6 (b). The same is true for $C_\sigma(r)$ while the pairing correlations, e.g. $C_a^\sigma(r)$ remain (small but) algebraic. The exponential suppression of the single-particle correlations may also be seen by the blurring of the momentum-distribution in that region as shown in Fig. 4 (c). So, hence, for the 2D-zig-zag ladder we may observe both a pair-SS phase (for $1/3 \gtrsim \rho \gtrsim 1/2$) as well as an ordinary SS phase.

Indeed, the presence of the pairing phase for the zig-zag ladder may be understood already from the Bose-Hubbard limit for a strong atom-photon coupling due to the presence of the solid phase at half filling $\rho = 1/2$ for $t \rightarrow 0$. In this limit one observes, that it is energetically favorable in a grand-canonical ensemble to dope the system with an even number of holes such that the total size of domain-wall excitations (in pairs of 3 lattice sites) become commensurate with the original crystalline lattice structure (4 lattice sites unit-cell). Hence we may understand the dominant pairing correlation observed numerically in the JCH-model on a zig-zag ladder as a reminiscent of this phase.

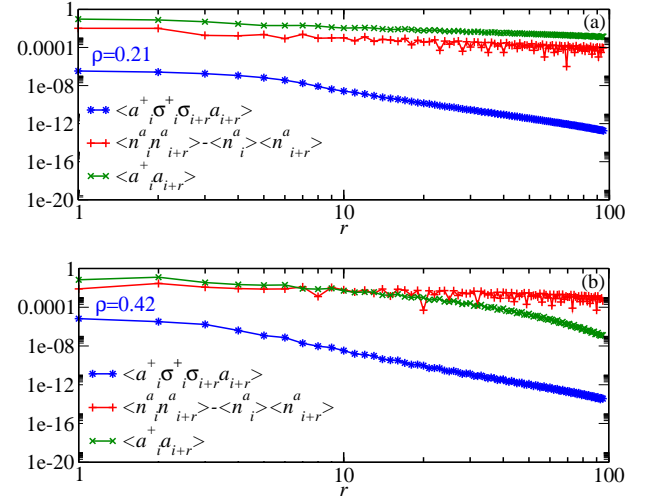


FIG. 6. DMRG method detailed description of the extended JCH model on the triangular zigzag ladder with $V/\beta = 0.4$, $t/\beta = 0.015$. (a) Power-law decaying of three correlations $C_a^\sigma(r)$, $C_n^\sigma(r)$, and $C_a(r)$ at $\rho = 0.21$. (b) Power-law decaying of $C_a^\sigma(r)$, $C_n^\sigma(r)$ and exponentially decaying of $C_a(r)$ at $\rho = 0.42$.

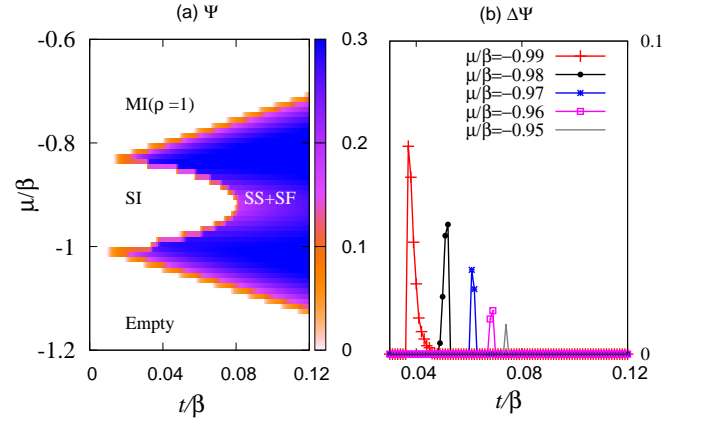


FIG. 7. Phase diagrams and the detailed description of $\Delta\Psi$ for 1D hardcore extended JCH model with $V/\beta = 0.4$ by the MF method. (a) The SF order Ψ . (b) The SS order $\Delta\Psi$ vs t/β with μ/β from -0.99 to -0.95 .

V. JCH MODEL ON ONE DIMENSIONAL LATTICES

A. Hardcore JCH model

We study the 1D hardcore extended JCH model, for which the results may be confirmed by the DMRG method. The maximum number of photons is restricted to be one in each cavity site. It is well known that the number of photons is not fixed in a grand canonical ensemble [21]. Therefore, the softcore photon system will be checked in the next section.

Fig. 7(a) shows the phase diagram as obtained from CMF-calculations, which contains the empty, SI, SS, SF and MI($\rho = 1$) phases, by plotting Ψ in the plane (t/β , μ/β). The SS phase exists in the tips around the SI phase. The phase diagram is not exactly symmetric with particle-hole symmetry at $\mu/\beta = -0.915$, which is a bit different from the case of hardcore bosons on bipartite lattices [49–51] as a result of the atom-photon coupling.

As t/β is small, and $\mu/\beta < -1$, the system is in an empty phase with $\rho = 0$ and $\Psi = 0$. While the system sits in the MI($\rho = 1$) phase if $\mu/\beta > -0.83$. Moreover, when $-0.99 < \mu/\beta < -0.84$, the SI phase appears. As t/β gets larger, the system enters the SF phase. As discussed in Ref. [12], for a large hopping t/β , the ground-state energy becomes negative and can be made arbitrarily small by increasing the total number of excitations. Herein, since the maximum number of photons is fixed, the SF remains stable.

In Fig. 7(b), we scan t/β along μ/β from -0.95 to -0.99 , $\Delta\Psi$ is obviously nonzero. The SS phase ($\Delta\Psi \neq 0$) emerges around the tips of the SI phase. A similar phase diagram of the JCH model has been obtained on the square lattice in Ref. [31]. The question about whether or not the SS phase could exist in the thermodynamic limit now can be verified by the DMRG method.

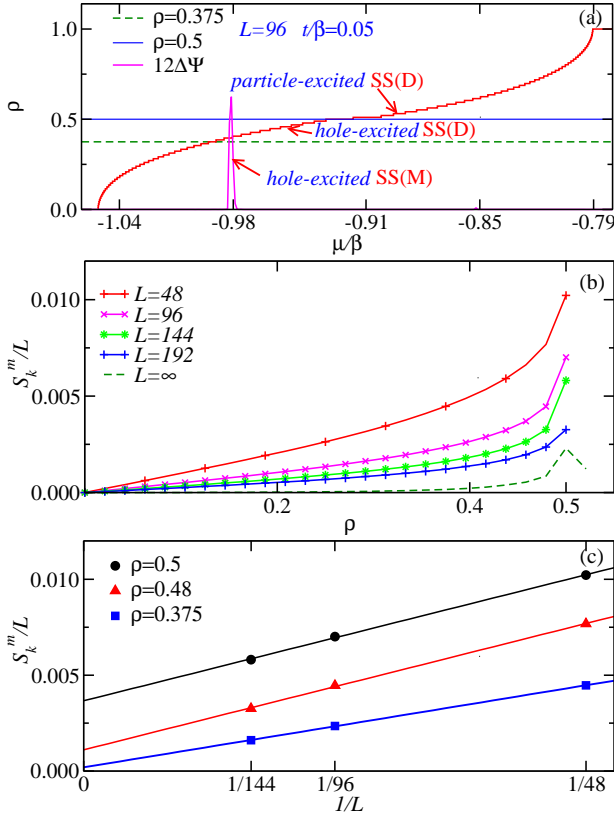


FIG. 8. DMRG method simulation of the 1D hardcore extended JCH model with $V/\beta = 0.4$, $t/\beta = 0.05$. (a) ρ vs μ/β with $L = 96$. (b) The structural factor S_k^m/L vs ρ . (c) Finite size scaling of S_k^m/L vs $1/L$, where $L = 48, 96, 144$.

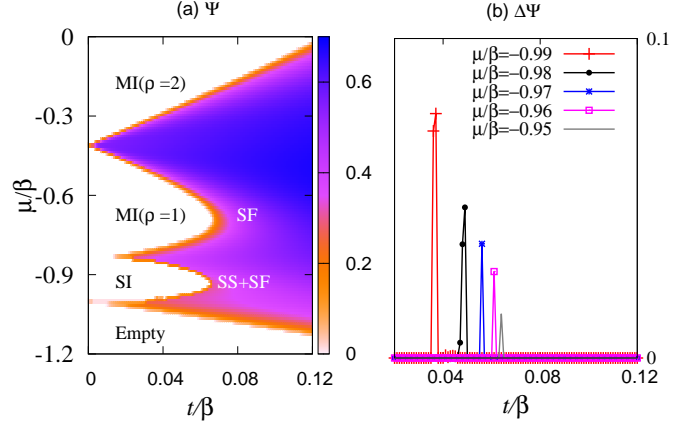


FIG. 9. Phase diagrams and the detailed description of $\Delta\Psi$ for 1D softcore extended JCH model with $V/\beta = 0.4$ by the MF method. (a) The SF order Ψ . (b) $\Delta\Psi$ vs t/β with μ/β from -0.99 to -0.95 .

In Fig. 8(a), the SI phase exists with $\rho = 1/2$ due to $V \neq 0$. Around the SI phase, the SS phase obtained by the DMRG calculation labeled by SS(D) exists in the range $0.375 < \rho < 0.5$. In previous works [7, 49], for the hardcore bosons, there was no any SS phase. The emergence of the SS phase of the JCH model is similar to that of Ref. [27], which is caused by hole-excitation. Particle-excited supersolid appears around 0.5 but larger than 0.5 (not shown). The SS phase of the MF method labeled by SS(M) exists around $\mu/\beta = -0.98$ as $\Delta\Psi$ is nonzero. To clearly present $\Delta\Psi$, we scale it up 12 times. Both methods support the SS phase.

The maximum structural factor S_k^m/L with sizes $L = 48, 96, 144$ are shown in Fig. 8(b). In Fig. 8(c), finite size scaling analysis of S_k^m/L at $\rho = 0.48$ shows that hole-excited SS phase exists in the thermodynamic limit but it is weak. The data of $\rho = 0.375, 0.5$ are for the purpose of reference.

B. Softcore JCH model

To check whether or not the results in the above section are stable without the hardcore constraint, we assume there are 2 photons at most in each cavity. Fig. 9(a) shows the MF phase diagrams, which contain the SF, SI, SS and MI($\rho = 1$) and MI($\rho = 2$) phases.

By comparing the results of the hardcore JCH model, we find that the consistent results are as follows: Firstly, only one SI phase emerges in the range $-0.975 < \mu/\beta < -0.87$. Secondly, the SS phase emerges only around the tip of the SI phase. In Fig. 9(b), by scanning t/β along μ/β from -0.95 to -0.99 , $\Delta\Psi$ is obviously nonzero, which indicates that increasing the occupation number of photons does not affect the emergence of the SS phase.

However, the SS phase only exists around the tip of

the SI phase and the area is relatively very narrow in the phase diagram. According to Refs. [52–54], a larger area of the SS phase appears if there is a strong interaction. For the JCH model, the SS phase does not obey this behavior even when V/β is very large. The reason is that the atom in each cavity only has two-level energies.

For the softcore Bose-Hubbard model on the bipartite lattice [45, 55–58], in the phase diagrams, there is more than one solid phase and the possible patterns of occupation numbers are (0, 1), (0, 2), (0, 3) and (1, 2) etc However, only one solid phase emerges in the JCH model. The absence of degeneracy between different solid phases hinder the formation large area of the SS phase.

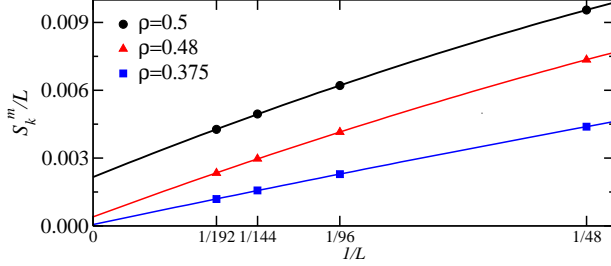


FIG. 10. Finite size scaling analysis of S_k^m/L from the 1D softcore extended JCH model at $V/\beta = 0.4$, $t/\beta = 0.05$ with $L = 48, 96, 144, 192$ by the DMRG method.

Fig. 10 shows the finite size scaling of S_k^m/L on the 1D softcore extended JCH model with sizes $L = 48, 96, 144, 192$ by the DMRG method, and the results prove that, without the hardcore constraint, the light supersolid still may exist.

C. Beats in the correlation and momentum distribution in the SS phase

The correlation $C_n^\sigma(r)$ and its Fourier transform S_k/L are also interesting quantities. We see beats or soliton patterns [45]. The non-diagonal correlation $C_a(r)$ and the momentum distribution $n(k)$ are also calculated. The SS phase with solitons has new features, which will be illustrated here.

In Fig. 11(a), we choose a point in the SS phase with $t/\beta = 0.05$, $\mu/\beta = -0.95$, with size $L = 128$. Interestingly, the atom excitation correlation $C_n^\sigma(r)$ emerges in the beats phenomenon [44], or the so-called solitons as in Ref. [45].

In Fig. 11(c), the Fourier transform of $C_n^\sigma(r)$, namely, S_k/L is shown. We find that around $k/\pi = 1$, two peaks emerge and are symmetric with $k/\pi = 1$. This means that the system enters into a solid order. The positions of the two peaks are located at $k_1/\pi = 1.17$ and $k_2/\pi = 0.83$, which satisfy the existence condition of the beats [44]. Actually, according to $\lambda_1 = 2$ and $\lambda_2 = 12$, we can also obtain k_1 and k_2 [59].

In Fig. 11(b), $C_a(r)$ is plotted and no beats form, which is a different outcome from our former work [44]. In

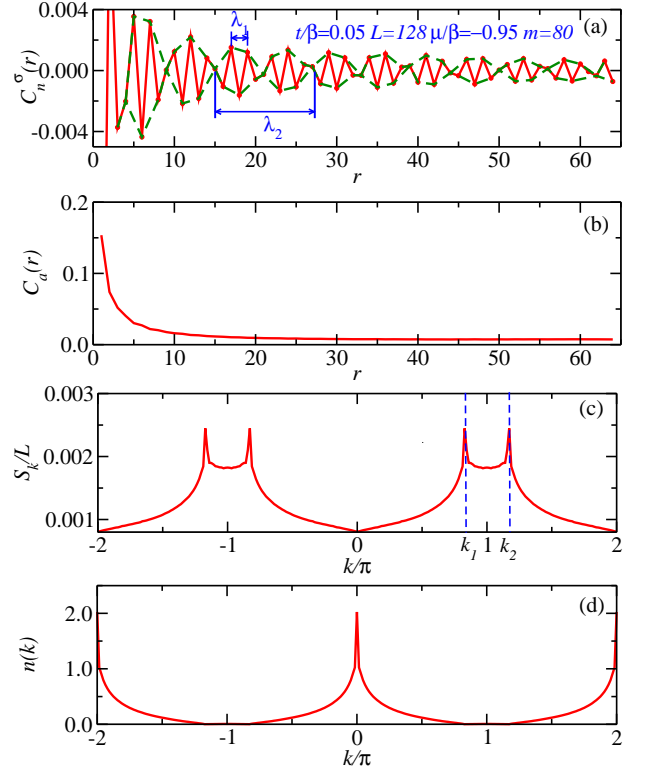


FIG. 11. (a) Correlation of the atom $C_a(r)$. (b) Correlation of the photon $C_n^\sigma(r)$. (c) Density structural factor S_k/L . (d) Momentum distribution with $\mu/\beta = -0.95$, $t/\beta = 0.05$, $L = 128$, and $m = 80$.

Fig. 11(d), the momentum distribution $n(k)$ emerges in a peak at $k = 0$, which indicates that the system has a SF order. Comparing with Fig. 11(c), the SS phase has both the SF order and the solid order, as expected.

In summary, the system is in a SS phase with beats or solitons. We also calculated the $C_n^\sigma(r)$ for the hardcore model, where the SS phase also emerges with beats.

VI. DISCUSSION AND CONCLUSIONS

Through a systematical study of the extended JCH model on the triangular and one dimensional lattices, we find that the light supersolid is stable in coupled cavities in the thermodynamic limit even when the photon hopping term is considered.

On the triangular lattices, in the phase diagram, apart from the hole-excited and particle-excited SS phase, we also see the additional SS phase. Obviously, the area of the supersolid is relatively wider than that in the one dimensional bipartite lattice, which is helpful to be detected experimentally.

For both the hardcore and softcore JCH models, using MF and the DMRG methods, we find the SS phases (hole-excited or particle-excited) exist around the tips of the solid phases.

It is worth mentioning, we find that the novel pair correlation caused by the interplay between the atoms in the cavities and the atom-photon interaction. On the other hand, the correlation in the SS phase emerges in the pattern of beats, or so-called solitons [45], by the reliable DMRG method.

For the formation of the SS phase of the Bose-Hubbard model, the key is the interaction, which is absent between photons. However, the solid and SS of photons still can form through the atom-photon coupling.

It may be interesting to test the possibility of existence of pair correlation, beats and supersolid in other atom-photon coupled systems in the future. Our results, obtained by MF and the DMRG methods, will be helpful

in the guiding experimentalists in realizing different and novel quantum phase on optical lattices.

ACKNOWLEDGMENTS

WZ and SG acknowledge hospitality of KITPC Beijing in August 2016 conference on the topic “Spin-orbit-coupled quantum gases”. We would like to thank T.C. Scott in helping prepare this document. S.G. acknowledges support of the Research Training Group (RTG) 1729 and project no. SA 1031/10-1 of the German Research Foundation (DFG). WZ is supported by the NSFC under Grant No.11305113.

-
- [1] O. Penrose and L. Onsager, Bose-Einstein Condensation and Liquid Helium, *Phys. Rev.* **104**, 576 (1956).
 - [2] G. V. Chester, Speculations on Bose-Einstein Condensation and Quantum Crystalline, *Phys. Rev. A* **2**, 256 (1970).
 - [3] A. J. Leggett, Can a Solid Be “Superfluid”?, *Phys. Rev. Lett.* **25**, 1543 (1970).
 - [4] M. H. W. Chan, R. B. Hallock, and L. Reatto, Overview on Solid ^4He and the Issue of Supersolidity, *J. Low. Temp. Phys.* **172**, 317 (2013).
 - [5] M. Greiner, O. Mandel, T. Dörslinger, T. W. Hänsch, and I. Bloch, Quantum phase transition from a superfluid to a Mott insulator in a gas of ultracold atoms, *Nature* **415**, 39 (2002).
 - [6] M. Greiner and S. Föllin, Optical lattices, *Nature* **453**, 736 (2008).
 - [7] M. Boninsegni, Phase Separation in Mixtures of Hard Core Bosons, *Phys. Rev. Lett.* **87**, 087201 (2001).
 - [8] A. B. Kuklov and B. V. Svistunov, Counterflow Superfluidity of Two-Species Ultracold Atoms in a Commensurate Optical Lattice, *Phys. Rev. Lett.* **90**, 100401 (2003).
 - [9] C. Trefzger, C. Menotti, and M. Lewenstein, Pair-Supersolid Phase in a Bilayer System of Dipolar Lattice Bosons, *Phys. Rev. Lett.* **103**, 035304 (2009).
 - [10] J. P. Lv, Q. H. Chen, and Y. J. Deng, Two-species hardcore bosons on the triangular lattice: A quantum Monte Carlo study, *Phys. Rev. A* **89**, 013628 (2014).
 - [11] F. Deppe, M. Mariani, E. P. Menzel, A. Marx, S. Saito, K. Kakuyanagi, H. Tanaka, T. Meno, K. Semba, H. Takayanagi, E. Solano, and R. Gross, Two-photon probe of the Jaynes-Cummings model and symmetry breaking in circuit QED, *Nature Phys.* **4**, 686 (2008).
 - [12] J. Koch and K. L. Hur, Superfluid-Mott-insulator transition of light in the Jaynes-Cummings lattice, *Phys. Rev. A* **80**, 023811 (2009).
 - [13] D. Underwood, W. Shanks, J. Koch, and A. Houck, Low-disorder microwave cavity lattices for quantum simulation with photons, *Phys. Rev. A* **86**, 023837 (2012).
 - [14] K. Toyoda, Y. Matsuno, A. Noguchi, S. Haze, and S. Urabe, Experimental Realization of a Quantum Phase Transition of Polaritonic Excitations, *Phys. Rev. Lett.* **111**, 160501 (2013).
 - [15] S. Schmidt, G. Blatter, and J. Keeling, From the Jaynes-Cummings-Hubbard to the Dicke model, *J. Phys. B: At. Mol. Opt. Phys.* **46**, 224020 (2013).
 - [16] G. Kailitis, F. Krüger, F. Nissen, and J. Keeling, Disordered driven coupled cavity arrays: Nonequilibrium stochastic mean-field theory, *Phys. Rev. A* **87**, 013840 (2013).
 - [17] C. Nietner and A. Pelster, Ginzburg-Landau Theory for the Jaynes-Cummings-Hubbard Model, *Phys. Rev. A* **85**, 043831 (2012).
 - [18] S. Schmidt and G. Blatter, Strong coupling theory for the Jaynes-Cummings-Hubbard model, *Phys. Rev. Lett.* **103**, 086403 (2009).
 - [19] A. Mering and M. Fleischhauer, Analytic approximations to the phase diagram of the Jaynes-Cummings-Hubbard model, *Phys. Rev. A* **80**, 053821 (2009).
 - [20] A. Souza, B. Sanders, and D. Feder, Fermionized photons in the ground state of one-dimensional coupled cavities, *Phys. Rev. A* **88**, 063801 (2013).
 - [21] M. Hohenadler, M. Aichhorn, S. Schmidt, and L. Pollet, Dynamical critical exponent of the Jaynes-Cummings-Hubbard model, *Phys. Rev. A* **84**, 041608 (2011).
 - [22] J. Z. Zhao, A. W. Sandvik, and K. Ueda, Insulator to superfluid transition in coupled photonic cavities in two dimensions, *arXiv:0806.3603*.
 - [23] A. L. C. Hayward, A. M. Martin, and A. D. Greentree, Fractional Quantum Hall Physics in Jaynes-Cummings-Hubbard Lattices, *Phys. Rev. Lett.* **108**, 223602 (2012).
 - [24] G. Almeida and A. Souza, Quantum transport with coupled cavities on an Apollonian network, *Phys. Rev. A* **87**, 033804 (2013).
 - [25] Y. L. Dong, S. Q. Zhu, and W. L. You, Quantum-state transmission in a cavity array via two-photon exchange, *Phys. Rev. A* **85**, 023833 (2012).
 - [26] J. Quach, Disorder-correlation-frequency-controlled diffusion in the Jaynes-Cummings-Hubbard model, *Phys. Rev. A* **88**, 053843 (2013).
 - [27] X. F. Zhang, Q. Sun, Y. C. Wen, W. M. Liu, S. Eggert, and A. C. Ji, Superradiant Solid in Cavity QED Coupled to a Lattice of Rydberg Gas, *Phys. Rev. Lett.* **110**, 090402 (2013).
 - [28] S. Wessel, and M. Troyer, Supersolid hardcore bosons on the triangular lattice *Phys. Rev. Lett.* **95**, 127205 (2005).
 - [29] M. Boninsegni, and N. Prokof'ev, Supersolid phase of hardcore bosons on triangular lattice, *Phys. Rev. Lett.* **95**, 237204 (2005).
 - [30] W. Z. Zhang, R. X. Yin, and Y. C. Wang, Pair super-

- solid of the extended Bose-Hubbard model with atom-pair hopping on the triangular Lattice, *Phys. Rev. B* **88**, 174515 (2013).
- [31] B. Bujnowski, J. Corso, A. Hayward, J. Cole, and A. Martin, Supersolid phases of light in extended Jaynes-Cummings-Hubbard systems, *Phys. Rev. A* **90**, 043801 (2014).
 - [32] T. D. Kühner, S. R. White, and H. Monien, One-dimensional Bose-Hubbard model with nearest-neighbor interaction, *Phys. Rev. B* **61**, 12474 (2000).
 - [33] T. Mishra, R. V. Pai, and S. Mukerjee, Supersolid in a one-dimensional model of hard-core bosons, *Phys. Rev. A* **89**, 013615 (2014).
 - [34] T. Mishra, S. Greschner, and L. Santos, Polar molecules in frustrated triangular ladders, *Phys. Rev. A* **91**, 043614 (2015).
 - [35] D. vanOosten, P. vanderStraten, and H. T. C. Stoof, Quantum phases in an optical lattice, *Phys. Rev. A* **63**, 053601 (2001).
 - [36] Y. Z. Ren, N. H. Tong, and X. C. Xie, Cluster mean-field theory study of J(1)-J(2) Heisenberg model on a square lattice, *J. Phys. Condens. Matter* **26**, 115601 (2014).
 - [37] D. Yamamoto, Correlated cluster mean-field theory for spin systems, *Phys. Rev. B* **79**, 144427 (2009). D. Yamamoto, G. Marmorini, and I. Danshita, Microscopic Model Calculations for the Magnetization Process of Layered Triangular-Lattice Quantum Antiferromagnets, *Phys. Rev. Lett* **114**, 027201 (2015).
 - [38] Dirk-Sören Lühmann, Cluster Gutzwiller method for bosonic lattice systems, *Phys. Rev. A* **87**, 043619 (2013).
 - [39] H. M. Deng, H. Dai, J. H. Huang, X. Z. Qin, J. Xu, H. H. Zhong, S. C. He, and C. H. Lee, Cluster Gutzwiller study of the Bose-Hubbard ladder: Ground-state phase diagram and many-body Landau-Zener dynamics, *Phys. Rev. A* **92**, 023618 (2015).
 - [40] S. R. White, Density Matrix Formulation for Quantum Renormalization Groups, *Phys. Rev. Lett.* **69**, 2863 (1992).
 - [41] U. Schollwoeck, The density-matrix renormalization group, *Rev. Mod. Phys.* **77**, 259 (2005).
 - [42] D. Heidarian and K. Damle, Persistent Supersolid Phase of Hard-Core Bosons on the Triangular Lattice, *Phys. Rev. Lett.* **95**, 127206 (2005).
 - [43] R. G. Melko, A. Paramekanti, A. A. Burkov, A. Vishwanath, D. N. Sheng, and L. Balents, Supersolid Order from Disorder: Hard-Core Bosons on the Triangular Lattice *Phys. Rev. Lett.* **95**, 127207 (2005).
 - [44] W. Zhang, S. Greschner, E. Fan, T. C. Scott, and Y. Zhang, Ground State Properties of the One-Dimensional Unconstrained Pseudo-Anyon Hubbard Model, arXiv:1609.02594v2.
 - [45] T. Mishra, R. V. Pai, and S. Ramanan, Supersolid and solitonic phases in the one-dimensional extended Bose-Hubbard model, *Phys. Rev. A* **80**, 043614 (2009).
 - [46] D. Yamamoto, I. Danshita, and C. A. R. Sa de Melo Dipolar bosons in triangular optical lattices: Quantum phase transitions and anomalous hysteresis, *Phys. Rev. A* **85**, 021601 (2012).
 - [47] Y. C. Wang, W. Z. Zhang, H. Shao, and W. A. Guo, Extended Bose-Hubbard model with pair hopping on triangular lattice, *Chin. Phys. B* **22** 96702 (2013).
 - [48] Y. C. Chen, R. G. Melko, S. Wessel, and Y. J. Kao, Supersolidity from defect condensation in the extended boson Hubbard model, *Phys. Rev. B* **77**, 014524 (2008).
 - [49] S. Wessel, Phase diagram of interacting bosons on the honeycomb lattice, *Phys. Rev. B* **75**, 174301 (2007).
 - [50] P. Sengupta, L. P. Pryadko, F. Alet, M. Troyer, and G. Schmid, Supersolids versus Phase Separation in Two-Dimensional Lattice Bosons, *Phys. Rev. Lett.* **94**, 207202 (2005).
 - [51] G. G. Batrouni and R. T. Scalettar, Phase Separation in Supersolids, *Phys. Rev. Lett.* **84**, 1599 (2000).
 - [52] M. Iskin, Route to supersolidity for the extended Bose-Hubbard model, *Phys. Rev. A* **83**, 051606 (2011).
 - [53] T. Ohgoue, T. Suzuki, and N. Kawashima, Commensurate Supersolid of Three-Dimensional Lattice Bosons, *Phys. Rev. Lett.* **108**, 185302 (2012).
 - [54] T. Ohgoue, T. Suzuki, and N. Kawashima, Ground-state phase diagram of the two-dimensional extended Bose-Hubbard model, *Phys. Rev. B* **86**, 054520 (2012).
 - [55] G. G. Batrouni, V. G. Rousseau, R. T. Scalettar, and B. Grmaud, Competing phases, phase separation, and coexistence in the extended one-dimensional bosonic Hubbard model, *Phys. Rev. B* **90**, 205123 (2014).
 - [56] G. G. Batrouni, R. T. Scalettar, V. G. Rousseau, and B. Grmaud, Competing Supersolid and Haldane Insulator Phases in the Extended One-Dimensional Bosonic Hubbard Model, *Phys. Rev. Lett.* **110**, 265303 (2013).
 - [57] J. M. Fellows, and S. T. Carr, Superfluid, solid, and supersolid phases of dipolar bosons in a quasi-one-dimensional optical lattice, *Phys. Rev. A* **84**, 051602 (2011).
 - [58] G. G. Batrouni, F. Hébert, and R. T. Scalettar, Supersolid Phases in the One-Dimensional Extended Soft-Core Bosonic Hubbard Model, *Phys. Rev. Lett.* **97**, 087209 (2006).
 - [59] B. Girod, R. Rabenstein and A. Stenger, Signals and Systems (Wiley, 2001).